

Relation between Photoacoustic Amplitude and Quenching of Mercury $^3P_1 \rightarrow ^1S_0$ Fluorescence by Hydrogen in Argon

J. E. Patterson

Chemistry Division, Department of Scientific and Industrial Research, Private Bag, Petone, New Zealand

The quenching of mercury fluorescence excited by a modulated low-pressure mercury vapour lamp causes sound to be developed in the quench gas. Apparatus has been developed which allows the simultaneous measurement of fluorescence and acoustic signals as a function of quench gas composition. The amplitudes of the fluorescence and acoustic signals sum to a constant over the range of quench gas compositions from 0.01 to *ca* 1%, by volume, of hydrogen in argon. Normalized amplitudes therefore sum to unity. Similar results are also obtained by substituting helium for argon. The normalized amplitude of the acoustic signal is related to quench gas composition by a modified Stern–Volmer equation. Provisional quench reaction rate constants obtained from acoustic data at 295 K, using this equation, compare well with rate constants obtained from fluorescence data and also with literature values.

Sound is produced in a silica cell containing mercury vapour and nitrogen irradiated by a modulated low-pressure mercury lamp at 253.7 nm. Substituting 1% hydrogen in argon by volume, for the nitrogen produces substantially greater acoustic signal amplitudes. The acoustic signal obtained is a consequence of the quenching of mercury fluorescence by a diatomic gas,¹ which causes some of the energy from the incident radiation to be degraded to heat. This in turn causes a pressure change in the sample cell. If the mercury lamp is modulated then an acoustic signal at the modulation frequency will be produced in the cell.

The recent development of a sensitive photoacoustic mercury analyser^{2,3} capable of detecting $< 10^{10}$ atoms of mercury, in a nitrogen carrier, has resulted in a need to explore the relationship between the quenching of mercury fluorescence and the amplitude of the acoustic signal. This may lead to improved quench-gas mixtures to maximize acoustic output, and to mixtures suitable for special applications such as field-portable instruments. The requirement is to release as much of the 469 kJ mol⁻¹, that the 253.7 nm mercury line represents, as heat while avoiding excessive losses to the cell wall. If this energy can be used to initiate other exothermic processes then the sound produced will be further enhanced.

If the mercury content in the cell is held constant and the concentration of a quench gas is changed in an inert carrier, such as argon or helium, then the acoustic and fluorescence signals vary in a complimentary and characteristic way. Equations relating fluorescence quenching to the pressure of quench gas in a sample cell have long been established^{4,5} and to some extent apply to real systems. The Stern–Volmer equation:

$$Y_f = \frac{1}{1 + \kappa P_Q} \quad (1)$$

which describes some fluorescence quenching processes, has been modified below to describe the amplitude of the acoustic signal produced as a function of added quench gas to an argon carrier. Y_f is the normalized fluorescence signal F/F_0 , F_0 being the fluorescence in the absence of quench gas, κ is the Stern-Volmer constant and P_Q is the pressure of quench gas. The proposed equation for the acoustic signal is

$$Y_s = 1 - \frac{1}{1 + \kappa P_Q} \quad (2)$$

where Y_s is the normalized acoustic signal S/S_0 , S_0 being the maximum signal obtained in a quenching experiment. P_Q is now the percentage quench gas in an argon carrier at atmospheric pressure. This equation is obtained from the proposition that

$$Y_f + Y_s = 1 \quad (3)$$

for a normalized system where no other process than fluorescence quenching causes gas heating, and thermal losses from the system are small.

An alternative form for eqn (2) is

$$Y_s = \frac{P_Q}{\kappa' + P_Q} \quad (4)$$

where $\kappa' = 1/\kappa$. This form yields κ' as an intercept when P_Q/Y_s is plotted against P_Q . This form is more suitable for data where $Y_s \rightarrow 1$. Taking both sides of eqn (4) from eqn (1) yields the equation for Y_f . The intercept κ' is small and therefore $\kappa (= 1/\kappa')$ is very sensitive to minor variations in experimental data.

In this paper the extent to which the amplitude of the normalized acoustic and fluorescence signals, produced in the system mercury-hydrogen-argon, can be described by eqn (3) is examined. Quenching curves of the acoustic amplitude obtained from resonance-irradiated mercury vapour *vs.* the percentage of hydrogen in argon are presented and are related, using the above equations, to fluorescence quenching curves obtained at the same time. Approximate quenching reaction rate constants are also presented. To assess the effect of the argon carrier on the quenching process, results are also presented for a hydrogen-helium quencher.

Experimental

The results were obtained using a single-cell version of a recently developed photoacoustic mercury analyser^{2,3} adapted (fig. 1) for continuous analysis and simultaneous observation of fluorescence. Modifications included a window assembly for the observation of fluorescence and a Wood's horn to provide a black background. Fluorescence was observed using a solar-blind photo-multiplier with a pinhole entrance aperture and two external masks and a field lens admitting only near paraxial light. With this arrangement the fluorescence signals, when quenched, fell to $< 0.01\%$ of the unquenched signals. The sound signals, when unquenched, fell to $< 3\%$ of the quenched signals, representing mainly an electronic offset, corrected during data analysis, and a small amount of residual sound.

The quench gas composition, expressed as a percentage hydrogen by volume in argon, was determined throughout the experiment using a computer-controlled Extranuclear SpectrEL mass spectrometer.⁶ Instrument settings were chosen to hold argon signals at $m/e = 20$ and $m/e = 40$ at a fixed ratio, and the hydrogen signal ($m/e = 2$) was compared with the argon 36 isotope signal. A gravimetrically prepared and certified pressurized gas mixture containing 0.2% hydrogen in argon was flowed through the cell at $0.15 \text{ dm}^3 \text{ min}^{-1}$ before and after each run. Three further standards containing 2.94, 3.51 and 4.52% hydrogen in argon were prepared on a gas-handling rig using pressure

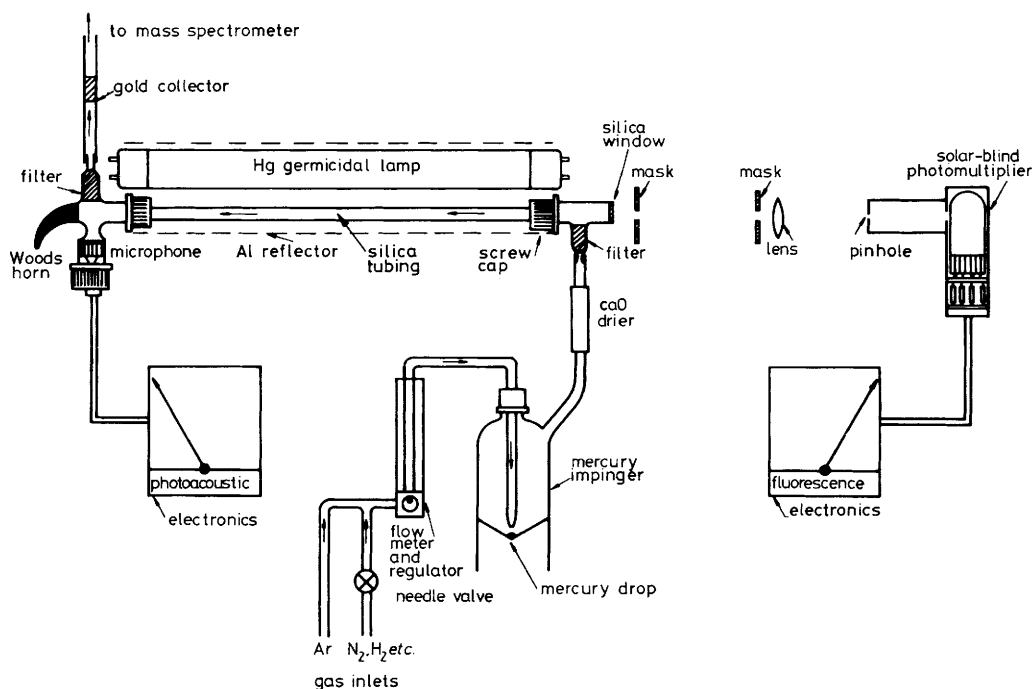


Fig. 1. Apparatus for monitoring the photoacoustic effect and fluorescence of mercury vapour as a function of quench gas composition.

ratios measured with a MKS Baratron digital pressure standard. Intercomparison of all the standards prepared gave calibration factors from 2.12 to 2.27%, averaging 2.2%. A 2.94% hydrogen in helium standard was also prepared with a calibration factor of 10.7%. Argon 36 was monitored during the experiment to allow correction for any slight drift in sensitivity during the run. The hydrogen $m/e = 2$ ion signal was ratioed with the argon $m/e = 36$ ion signal and multiplied by the calibration factor to determine the percentage of hydrogen by volume. Preamplified sound and fluorescence signals were monitored using two spare analogue-to-digital converter inputs in the mass-spectrometer control unit.

A mercury impinger⁷ made from Pyrex glass was used to provide a steady concentration of mercury vapour in the carrier gas at $ca. 0.4 \text{ ng cm}^{-3}$ or $1.2 \times 10^{12} \text{ atom cm}^{-3}$. The principle of this device was to direct a gas flow at a 1 mm diameter drop of mercury held in a conical depression. An initially high equilibrium concentration of mercury vapour rapidly fell to a steady level and thereafter fell by only a few percent over a period of days. Since the quenching experiments occupied a time usually $< 60 \text{ min}$, the mercury concentration could be considered static. Room temperature variations of $\pm 0.5 \text{ K}$ caused changes of $\pm 4\%$ in mercury concentration. This was minimized but not fully compensated for by insulating the impinger and, in one experiment, disabling the cycling of the room air conditioning. After prolonged use the mercury drop was cleaned by rolling it over the conical glass surface a few times.

The mercury concentration in the cell was measured by taking an aliquot and determining the concentration with a calibrated photoacoustic mercury detector. The concentration determined at 0.4 ng cm^{-3} was well within the normal acoustic linear working range of the instrument, as well as being reasonably linear for fluorescence. Flow control at $0.15 \text{ dm}^3 \text{ min}^{-1}$ was obtained using a capillary flow meter. Residual

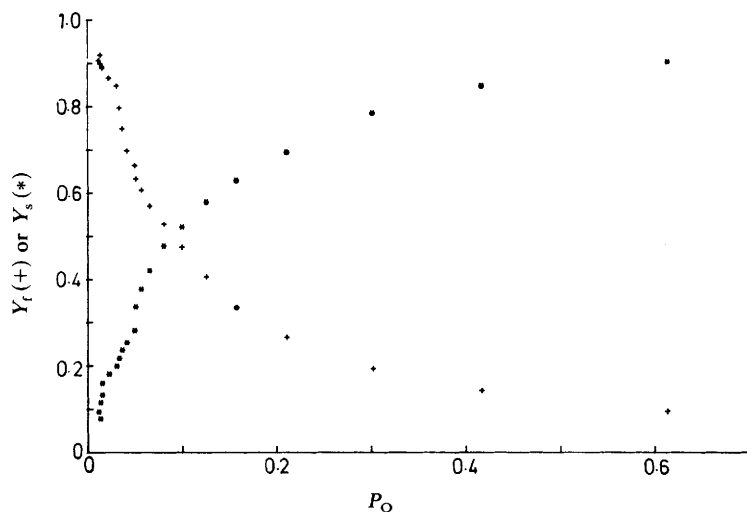


Fig. 2. Normalized fluorescence Y_f (+) and normalized acoustic amplitude Y_s (*) vs. percentage hydrogen in argon (P_Q) at 295 K (expt 1).

oxygen in the argon was removed with a heated copper catalyst. Hydrogen was added *via* a needle valve (fig. 1) set to maintain 2 or 3% hydrogen in argon. Shutting off the hydrogen valve in the laboratory gas distribution system provided a reserve of hydrogen in the connecting line, which fell in pressure over the 60–80 min duration of the experiment. The partially opened needle valve allowed the hydrogen to diffuse slowly into the argon carrier gas covering a wide range of compositions as it depleted. The change of hydrogen concentrations could not be allowed to occur too rapidly as there was a transit time of a few seconds from the photoacoustic cell to the mass spectrometer. Since quenching was complete at relatively low percentages of hydrogen in argon the total flow was nearly constant at $0.15 \text{ dm}^3 \text{ min}^{-1}$.

Results and Discussion

Fig. 2 shows normalized quenching curves for the fluorescence signal Y_f (where $Y_f = F/F_0$) and for the acoustic signal Y_s (where $Y_s = S/S_0$) vs. the percentage of hydrogen, P_Q , in argon. F_0 and S_0 were obtained by plotting the acoustic signal vs. fluorescence and determining the intercepts of the regression line ($r = 0.991$). The amplitude of the acoustic signal fell slightly at high percentages of hydrogen, probably reflecting changes in bulk properties such as a rising heat capacity and a rising thermal conductivity for hydrogen relative to argon, increasing losses to the walls. Note also the slight deviation from a smooth curve near 0.06% hydrogen in argon caused by a change in room temperature of *ca.* 0.5 K.

The data obtained in these experiments were evaluated using the Stern-Volmer equations above. It is acknowledged that the criteria of no radiation trapping and no Lorentz broadening may not be fully met here,⁸ but the equations can still be used to demonstrate the equivalence of the acoustic and fluorescence results. Plotting $1/Y_f$ and $1/(1 - Y_s)$ vs. P_Q (fig. 3) produces similar and near-linear regressions for values of $P_Q < \text{ca. } 0.7\%$ and deviations above this level. Here the quenching curves (fig. 2) have nearly levelled out causing larger errors where Y_f and $1 - Y_s$ are small.

An alternative was to use eqn (4) and plot $P_Q/(1 - Y_f)$ and P_Q/Y_s vs. P_Q (fig. 4). This resulted in a linear response over a wide range of hydrogen concentrations. κ'

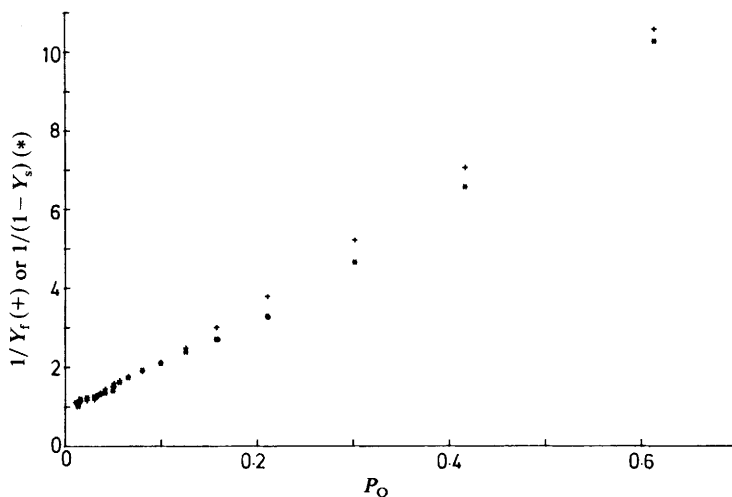


Fig. 3. Stern-Volmer derived plot of $1/Y_f$ (+) and $1/(1-Y_s)$ (*) vs. percentage hydrogen in argon (P_Q) at 295 K. Points above 0.7% hydrogen in argon are not plotted since Y_f and $1-Y_s \rightarrow 0$.

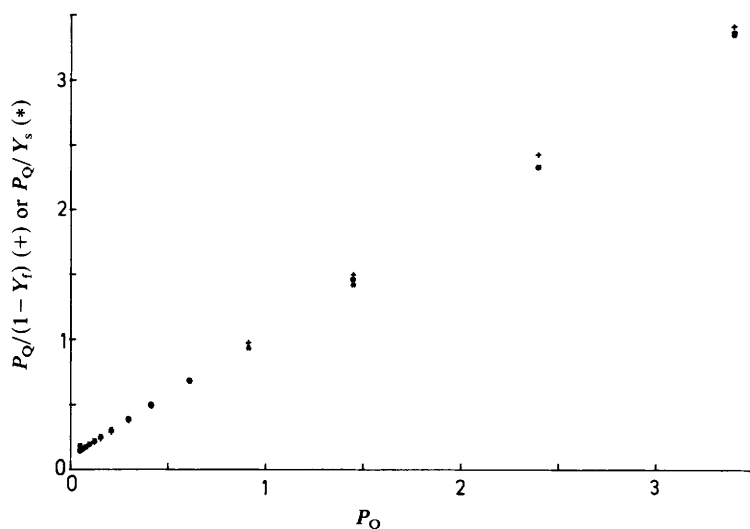


Fig. 4. Alternative Stern-Volmer derived plot of $P_Q/(1-Y_f)$ (+) and P_Q/Y_s (*) vs. percentage hydrogen in argon (P_Q) at 295 K. Points below 0.05% hydrogen in argon are not plotted since $1-Y_f$ and $Y_s \rightarrow 0$.

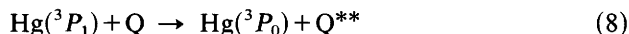
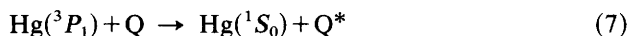
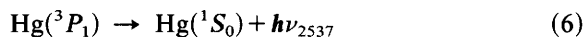
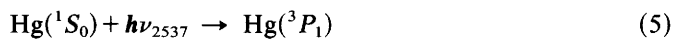
($=1/\kappa$) is now the value of the y intercept and the slope is near 1, and κ' can be obtained from a linear regression after deleting some end points where Y_s and $1-Y_f$ are either very small or constant. The y intercepts both for the fluorescence and acoustic signals are similar, and generally yielded values for κ a little lower than those obtained with eqn (2) (table 1). The differences are almost certainly due to differences in statistical weighting caused by the uneven distribution of points along the line and the sensitivity of the intercept to small errors in slope estimation. Repeating the experiments several times yielded consistent results using eqn (1) and (2) but more variation using eqn (4) (table 1, expt 3).

Table 1. Comparison between quenching constants obtained in argon and helium at 295 K for experiments 1 to 3 and 299 K for experiments 4 using the slope or intercept versions of the Stern-Volmer equation (κ can be multiplied by $3.1 \times 10^{-11} \% \text{ cm}^3 \text{ molecule}^{-1} \text{ s}^{-1}$ to obtain k_7)

mode	equation	$\kappa (\%^{-1})$ experiment no.				gas
		1	2	3	4	
sound	slope	14.5	15.4	14.5	11.4	argon
fluorescence	slope	15.4	14.5	14.9	9.5	argon
sound	intercept	9.2	9.3	10.3	9.9	argon
fluorescence	intercept	9.2	9.2	49	9.7	argon
sound	slope	14.5				helium
fluorescence	slope	15.9				helium
sound	intercept	8.6				helium
fluorescence	intercept	9.2				helium

Because of the nature of the quenching curves where the response levels out at *ca.* 1% hydrogen in argon, it should be noted that Stern-Volmer relationships will show deviations from linearity caused by systematic and random errors dominating as $Y_s \rightarrow 1$ and $Y_f \rightarrow 0$.

If the following general reactions⁹ describe the fluorescence quenching process:



where Q is the quench molecule, then the quenching constant κ is the ratio of the rate constants k_7 and k_6 of eqn (7) and (6). Values for k_6 have been obtained directly,^{10,11} with the main experimental problem being that of radiation trapping. Mercury atom densities $< 10^{12} \text{ atom cm}^{-3}$ appear to be necessary. The atom density in these experiments was $< 1.2 \times 10^{12} \text{ atom cm}^{-3}$, and the calibration of the equipment for acoustic amplitude and fluorescence was linear at this concentration. A value for k_6 of *ca.* $8.2 \times 10^6 \text{ s}^{-1}$ is therefore appropriate.¹⁰

From the acoustic data (table 1, expt 1) a value for k_7 of $4.5 \times 10^{-10} \text{ cm}^3 \text{ molecule}^{-1} \text{ s}^{-1}$ was obtained from κ and k_6 , where κ was determined from the regression slope of a Stern-Volmer plot (fig. 3, $r = 0.982$) at 295 K. From the fluorescence data a value for k_7 of $4.8 \times 10^{-10} \text{ cm}^3 \text{ molecule}^{-1} \text{ s}^{-1}$ was obtained at 295 K ($r = 0.996$). The values obtained for k_7 compare well with other values in the literature.^{12,13}

Using the intercept version of the Stern-Volmer equation a value for k_7 of $2.9 \times 10^{-10} \text{ cm}^3 \text{ molecule}^{-1} \text{ s}^{-1}$ was obtained from both the fluorescence and acoustic data (table 1, expt 1) ($r = 0.999$ for both lines).

Substituting a helium carrier for argon produced similar results ($\kappa = 4.5 \times 10^{-10} \text{ cm}^3 \text{ molecule}^{-1} \text{ s}^{-1}$ for the acoustic data and $4.9 \times 10^{-10} \text{ cm}^3 \text{ molecule}^{-1} \text{ s}^{-1}$ for the fluorescence data), showing that the presence of argon or helium did not influence the results greatly when compared with more classical experiments where low pressures are employed. The quenching constants from all experiments are summarized in table 1. Plotting Y_s vs. Y_f gave a line of slope -1 and an intercept of 1 with $r = 0.991$ (normalization ensured the integer values of slope and intercept).

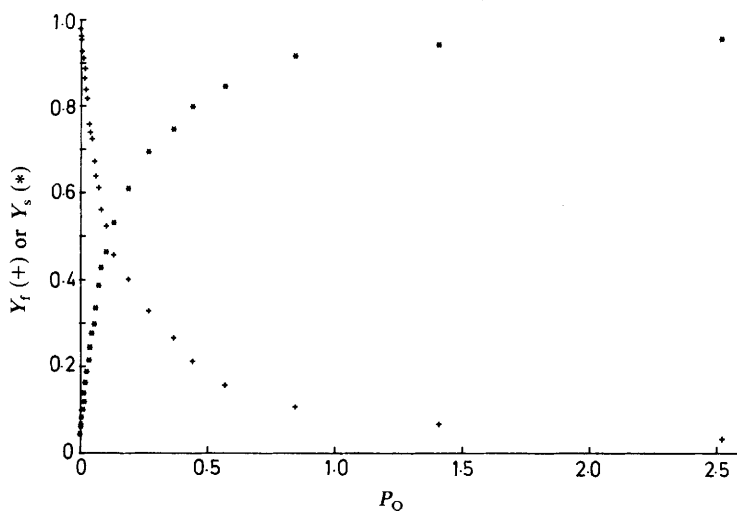


Fig. 5. Normalized fluorescence Y_f (+) and normalized acoustic amplitude Y_s (*) vs. percentage hydrogen in argon (P_Q) at 299 K (expt 4).

The main source of error in these experiments was temperature variation affecting the vapour pressure of mercury by $8\% \text{ K}^{-1}$. Insulation of the impinger was necessary. Running the experiment over shorter time intervals of *ca.* 10 min, by reducing the size of the hydrogen reservoir, improved the relationship between Y_s and Y_f ($r = 0.999$), but the determination of hydrogen concentrations was in error because of the time delay between the experiment and the mass spectrometer. This was not easy to correct for reliably hence the experiment time was lengthened to 60 min as a compromise. An attempt was made to obtain more constant temperature conditions by switching off the room air conditioning and allowing the room to equilibrate at mid-afternoon. The room heated to 299 K and stabilized. The corrected data yielded for Y_s vs. Y_f a correlation coefficient $r = 0.997$ but slightly lower values for κ (table 1, expt 4). The normalized quenching curves for this experiment are shown in fig. 5, and when compared with fig. 2 they demonstrate the effect of better temperature stabilization.

This work has established the relationship between the photoacoustic effect and the quenching of mercury fluorescence, by hydrogen in argon, when using a modulated light source. It has also been shown that photoacoustic observations may be used to obtain useful information about quenching processes which are equivalent to those obtained by fluorescence methods. This is consistent with previous work¹⁴⁻¹⁶ for absorption of light by organic molecules.

Further work is necessary to produce optimum performance from photoacoustic mercury analysers.^{2,3} For example, nitrogen is currently used as a quench gas, and detection limits $< 0.01 \text{ ng}$ mercury are obtainable. With 1% hydrogen in argon the signal is 4.3 times stronger than in nitrogen and 3.25 times stronger than in nitrogen with 1% hydrogen. The presence of residual oxygen may complicate any explanation of these results, but it may be that nitrogen increases the yield of mercury in the 3P_0 state [eqn (8)], which has a sufficiently long lifetime to increase the proportion of quenching at the walls, thus causing some heat loss from the system which is not observed as sound.

Prof. N. F. Curtis and Drs G. R. Burns, W. C. Tennant and J. Pearce are thanked for their interest in this work. Dr W. H. Melhuish is thanked for advice on a suitable notation. Mrs L. M. Parker is thanked for help with the mass spectrometry.

References

- 1 P. I. Bresler and B. N. Ruzin, *Opt. Spektrosk.*, 1956, **1**, 387.
- 2 J. E. Patterson, *Anal. Chim. Acta*, 1982, **136**, 321.
- 3 J. E. Patterson, *Anal. Chim. Acta*, 1984, **164**, 119.
- 4 O. Stern and M. Volmer, *Phys. Z.*, 1919, **20**, 183.
- 5 M. W. Zemansky, *Phys. Rev.*, 1930, **36**, 919.
- 6 L. M. Parker and J. E. Patterson, 1983, Report CD 2330, Chemistry Division, Department of Scientific and Industrial Research, Lower Hutt, New Zealand.
- 7 F. Aldrighetti, G. Carelli, A. Iannaccone, R. La Bua and V. Rimatori, *Atom Spectrosc.*, 1981, **2**, 13.
- 8 A. G. Mitchell and M. W. Zemansky, *Resonance Radiation and Excited Atoms* (Cambridge University Press, London, 1934).
- 9 J. V. Michael and G. N. Suess, *J. Phys. Chem.*, 1974, **78**, 482.
- 10 J. A. Halstead and R. R. Reeves, *J. Quantum Spectrosc. Radiat. Transfer*, 1982, **28**, 289.
- 11 L. F. Phillips, *J. Photochem.*, 1976, **5**, 277.
- 12 J. S. Deech, J. Pitre, and L. Krause, *Can. J. Phys.*, 1971, **49**, 1976.
- 13 T. Hikida, M. Santoku and Y. Mori, *Rev. Sci. Instrum.*, 1980, **51**, 1063.
- 14 L. M. Hall, T. F. Hunter and M. G. Stock, *Chem. Phys. Lett.*, 1976, **44**, 145.
- 15 T. F. Hunter, D. Rumbles and M. G. Stock, *J. Chem. Soc., Faraday Trans. 2*, 1974, **70**, 1010.
- 16 V. Upadhyaya, L. B. Tiwari and S. P. Mishra, *Spectrochim. Acta, Part A*, 1985, **41**, 833.

Paper 6/234; Received 3rd February, 1986